C. R. Mecanique 341 (2013) 715–725

Contents lists available at ScienceDirect

Comptes Rendus Mecanique

www.sciencedirect.com

2D axisymmetric X-FEM modeling of the Hertzian cone crack system

David Y. Tumbajoy-Spinel [a], Éric Feulvarch [b], Jean-Michel Bergheau [b], Guillaume Kermouche [a,*]

[a] *École nationale supérieure des mines de Saint-Étienne, centre SMS, LGF UMR CNRS 5307, 158 cours Fauriel, 42023 Saint-Étienne cedex 2, France*

[b] *Université de Lyon, ENISE, LTDS, UMR5513 CNRS, 58 rue Jean Parot, 42023 Saint-Etienne cedex 2, France*

ARTICLE INFO

Article history:
Received 26 July 2013
Accepted after revision 12 September 2013
Available online 22 October 2013

Keywords:
Cone crack
Indentation
Brittle materials
X-FEM
Silicate glasses
Contact

Mots-clés :
Fissuration en cône
Indentation
Matériaux fragiles
X-FEM
Verres silicatés
Contact mécanique

ABSTRACT

Hertzian cone cracks are nowadays a scholarly case making it possible to understand fracture of materials. However, the simulation of this physical phenomenon is not trivial and most theoretical models lead to the prediction of cone crack angles different from those observed experimentally. In the past, finite-element models have been developed based on a re-meshing procedure to explain this difference successfully, but with some limitations due the algorithms used. In this paper, we propose to use the X-FEM method to model Hertzian cone crack propagation with a 2D axisymmetric approach. The effect of various numerical parameters, such as mesh size or time step, is investigated and it is shown that they do not have a great impact on the crack angle result. The analysis of the stress field induced leads us to understand the difference in terms of cone crack angle based on the pre-existing stress field and those experimentally observed. As a conclusion, X-FEM is very efficient to reproduce faithfully several characteristics of the Hertzian cone crack phenomenon in a very simple manner.

RÉSUMÉ

La génération de fissures hertziennes de forme conique par des contacts mécaniques apparaît souvent comme un cas d'école pour étudier la rupture des matériaux fragiles. Cependant, la simulation de ce phénomène physique n'est pas triviale, car la plupart des modèles analytiques prédisent des angles de fissuration différents de ceux observés expérimentalement. Cette différence a pu être expliquée par des modélisations éléments finis reposant sur des algorithmes de remaillage très spécifiques, engendrant malheureusement un certain nombre de limitations pratiques. Dans cet article, nous proposons d'utiliser la méthode des éléments finis étendus pour représenter ce phénomène. L'angle de propagation obtenu est en très bon accord avec les résultats de la littérature, et la différence observée avec les modèles analytiques peut s'expliquer par une modification du champ de contraintes au cours de la propagation. Nous montrons aussi que les résultats obtenus sont robustes, c'est-à-dire qu'ils ne dépendent pas ou très peu de paramètres numériques tels que la taille des éléments ou la longueur d'extension de fissure. En conclusion, la technique X-FEM apparaît comme très efficace et suffisamment précise pour modéliser la rupture en cône de Hertz.

* Corresponding author.

1631-0721/$ – see front matter
http://dx.doi.org/10.1016/j.crme.2013.09.004

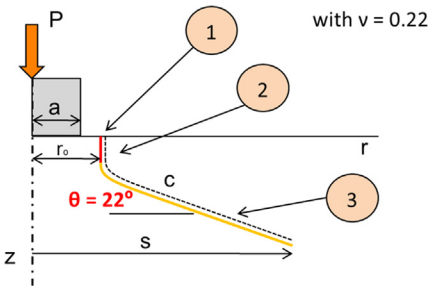

Fig. 1. Steps and parameters observed on the Hertzian cone crack development. Color online.

1. Introduction

Since the beginning of the 20th century, fracture mechanics has become an essential discipline to predict the behavior of several components in different industry domains. Then, the analysis of some general properties and the validation of certain methods used to estimate the fracture phenomenon were first studied from particular cases of crack propagation, such as the Hertzian cone system (Fig. 1).

Many researchers were interested to develop a number of experimental and analytical descriptions of the Hertzian cone, because this indentation system offers several advantages: firstly, the experimental test is reproducible, secondly, the crack path seems to be well defined and predictable, and finally the influence of several parameters on crack generation is almost known [1–15]. As a consequence, the Hertzian cone indentation is considered as a scholarly case to illustrate the generalities and characteristics of the crack growth phenomenon.

Nevertheless this apparent simplicity is misleading. Thanks to a finite-element analysis based on a specific re-meshing procedure, Kocer et al. [4] have particularly shown that the crack path predicted by the Hertzian analytical stress field is erroneous. This result is of primary importance concerning the analysis of this scholar case, but it seems to have been ignored during the past fifteen years. In our opinion, the main reason lies in the difficulty to establish a re-meshing procedure making it possible to predict with enough accuracy the stress field around a moving crack. The purpose of this paper is to show that the use of the Extended Finite-Element Method [16] is a good alternative to re-meshing-based methods to predict Hertzian cone cracks.

Firstly, the experimental and analytical considerations of the Hertzian cone system and a brief specification of the numerical simulation approach used by Kocer et al. [4,9] are detailed. Secondly, a general description of the X-FEM technique and its application to the particular case of the Hertzian cone system is presented with a 2D axisymmetric approach. Finally, the effect of various numerical parameters, such as mesh size or time step, is investigated. The results of the simulations performed with this technique – cone crack angle, stress field and energy release rate – are discussed in the last part of this paper.

2. About Hertzian cone cracks

The studies produced by Hertz in the 19th century proved that indentation tests performed with a spherical or flat punch on the surface of a fragile material lead to the development of an axisymmetric cone crack around the contact area. Fig. 1 shows a representation of the Hertzian cone, where the three general steps observed in the formation of the cone are illustrated.

Firstly, the superficial flaws placed around the indenter start growing under the influence of the flat punch pressure (*step 1*). When the stress field is high enough, the initial flaws get together to become an annulus crack. This crack starts growing orthogonally to the material surface in a concentric position with respect to the indenter axis (*step 2*) [10]. Finally, when the annulus is well formed, the crack starts growing as an axisymmetric cone with a constant angle usually defined as $\vartheta = 22°$, when $\nu = 0.21$ (*step 3*). According to several studies [2,6], a well-formed cone is obtained in a stable equilibrium, and its base radius depends on the load applied on the indenter ($s \propto P^{2/3}$). In Fig. 1, a is the indenter radius, c is the crack length and r_o is the annulus crack radius [5,11].

It should be remarked that brittle materials as Soda – lime glass or borosilicate glass – are characterized by a Young modulus $E = 70\,000$ MPa and $\nu = 0.21$. The indenter is a hardened steel flat punch with $E = 210\,000$ MPa, $\nu = 0.33$, and diameters ranging from 0.4 mm to 6.35 mm [6].

The analytical description of the Hertzian cone crack is always based on fracture mechanics general principles. The first important consideration in this domain is the representation of the crack in order to develop a reliable and simple model. Basically, in this case, the crack geometry is determined as the union of two independent crack surfaces named $\Gamma+$ and $\Gamma-$ respectively, where its intersection is known as the crack tip. The crack geometry is represented in Fig. 2.

In linear elastic fracture mechanics, the stress field is described by the Irwin relation, defined as a linear combination of the solutions associated with the three possible load configurations that can generate crack propagation. Mode I is a load applied in a normal direction to the crack plane, while modes II and III are forces applied in a tangential direction to the

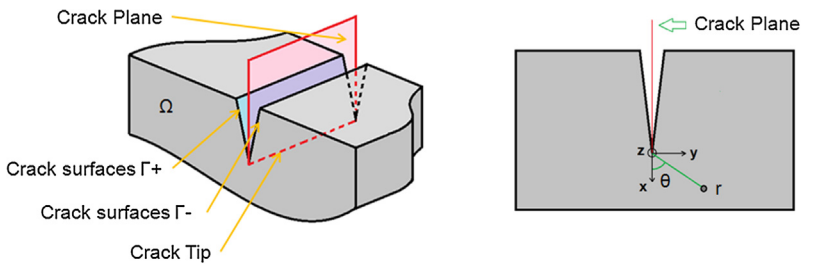

Fig. 2. Crack geometry and the coordinate system at the crack tip. Color online.

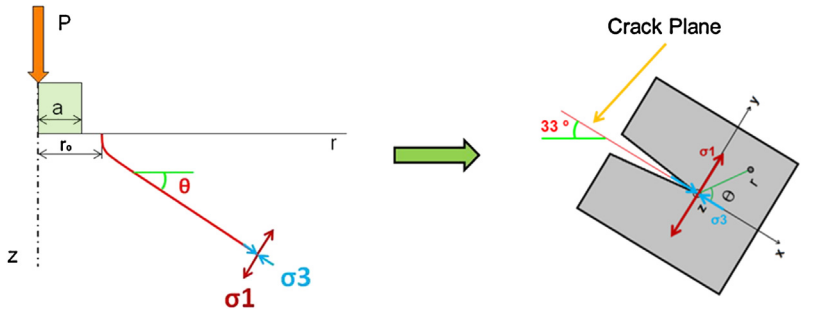

Fig. 3. Propagation of the Hertzian cone crack following the pre-existing trajectory of the principal stress σ_3. Color online.

crack plane. Moreover, each load mode is associated with a stress intensity factor (K_1, K_2, and K_3), which is considered as a parameter that reflects the influence of each load configuration on the development of the stress field around the crack tip [12].

Furthermore, fracture mechanics proposes a crack propagation criterion based on the strain energy release rate G. This factor corresponds to the relation between the energy variations in the material when a new free surface is generated by propagation. In general terms, when G becomes higher than a critical value G_c, crack propagation starts. Likewise, the crack growth direction is defined by the angle ϑ that maximizes the $G(\theta)$ value around the crack tip [13,14].

Following those general principles, several authors analytically defined the Hertzian cone and proposed several hypotheses and conclusions. One of the most remarkable assumptions made in the past is that the crack path is always defined by the pre-existing principal stress field, which means that the Hertzian cone crack coincides with the trajectory of the minimal principal stress σ_3 (Fig. 3). Knowing that the principal stresses are orthogonal, this supposition entails that σ_1 produces crack propagation under the effect of the *mode I*, considering this load as the only one that can produce crack growth. It must be mentioned that σ_2 is oriented perpendicularly to the figure plane [2,5,7].

This theory is based essentially on two arguments: (1) the analytical definition of the stress field shows that the geometry of the σ_3 trajectories is very similar to that found experimentally in the Hertzian cone crack system; (2) the estimation of the principal stress isovalues reveals that σ_1 is the only tensile stress near to the surface region where the crack is generated and propagates. As a result, the other principal stresses do not contribute to the crack extension [2,5,7].

This characterization of the Hertzian cone was strongly supported by several researches in the past; however more recent works, such as those presented by Kocer [1,4,9,15], expose several inconsistencies between the experimental results, the description presented by the analytical methods, and the solutions that he obtains using the numerical simulation of the crack propagation. In his work, Kocer estimates the angle of the cone crack path and compares it with the distribution of the pre-existing principal stress σ_3. Then he observes that the angles are very different for the same Poisson ratio ($\nu = 0.21$): 22° is obtained from the finite-element analysis, whereas 33° was predicted by the Hertzian analytical solution.

Therefore, the results found by Kocer point out two main contradictions between the numerical and the analytical methods in the description of the Hertzian cone. The first remark is that the cone angle value obtained analytically (22° for $\nu = 0.33$) differs considerably from that found with the numerical simulation; incidentally, the numerical solution presents very accurate results in accordance with the experimental tests [7,9]. The second contradiction is related to the divergence observed between the angles determined for the crack and the pre-existing stresses. Kocer's work reveals that the cone crack does not follow the pre-existing stress trajectories because their orientations are different, contrary to the hypothesis initially proposed by several authors in the past. Furthermore, he proposed that the pre-existing principal stresses trajectories evolve gradually from 33° to 22°, because of the continuous cone crack growth [4,9].

Consequently, in order to prove the performance of the X-FEM method in the computation of the Hertzian crack growth phenomenon, the works of Kocer et al. [4,9] could be taken as a pattern to develop a similar approach using another computation method. The finite-element model used by Kocer et al. is based on the re-meshing procedure of a cylindrical axisymmetric model for each iteration step. A constant meshing patch ahead of the crack tip is used in order to avoid a

random mesh structure in this zone, thus leading to minimize numerical uncertainties [4]. The stress intensity factors (SIFs) and the strain energy release rate G are employed in the crack propagation criterion and the crack growth direction ϑ of the next iteration is determined. Finally, the current position of the crack tip is updated. The main drawbacks of this re-meshing-based method are the high computational-time cost induced and the difficulty related to the mesh calibration at each iteration step. This is the reason why the X-FEM method, which does not require re-meshing algorithms [16], could be an interesting and efficient alternative to model Hertzian cone crack propagation.

3. General description of the X-FEM

One strong advantage of the X-FEM technique over the re-meshing-based procedure is that it is simpler to implement. Indeed, the crack is implicitly considered in the approximation of displacements and deformations. Some terms are added to the classical FEM approximation of displacements, without modifying the topology of the mesh. These enrichment terms depend on the geometry of the crack, which is modeled within a level set framework. The X-FEM approximation of the displacements can be written as follows [16]:

$$\mathbf{U} \approx \sum_{i=1}^{N} N_i \mathbf{u}_i + \sum_{j \in M} N_j H \mathbf{a}_j + \sum_{k \in T} N_k \left(\sum_{l=1}^{4} f_l \mathbf{b}_{kl} \right)$$

In these expressions, N denotes the number of nodes and N_i the shape function associated with node i. H and f_l are the enrichment functions. $\mathbf{u}_i$, $\mathbf{a}_j$ and $\mathbf{b}_{kl}$ denote the vectorial unknowns at each node. M is the subset of nodes whose support is cut by the crack. There are several ways to build the subset T corresponding to enrichment near the crack tip. For geometrical enrichment, T is composed of the subset of nodes whose distance is less than a length L characterizing the size of the area of K-dominance. The enrichment technique used in this work is topological. T is defined with the set of nodes whose support contains the crack tip [17].

The enrichment functions are not developed in this work because these are functions that are commonly used in classical cases of 3D studies with a plane strain assumption near the crack tip for the determination of SIFs. Moreover, the simulations correspond to a 3D modeling even if computations are 2D axisymmetric. This approach has been checked in the recent work of Tran and Geniaut [18].

At each time step, the stress and strain distributions are computed with the X-FEM approximation. The stress intensity factors, K_1 and K_2, are then computed via interaction integrals [19]. The misorientation angle of the crack is obtained from the criterion of maximum normal stress[1] and the feed pitch of the crack is defined a priori. At each step of the propagation, the level sets are updated following the procedure proposed by Stolarska et al. [20,21]. Thereby, the flow diagram in Fig. 4 illustrates an overall representation of the algorithm used in this work.

4. Simulation of the Hertzian cone using the X-FEM

In the flow diagram in Fig. 4, one may observe several characteristics of the algorithm, which differ from the computation method used by Kocer. Firstly, as was already mentioned, we note that the same mesh is used during the crack propagation; it is not here necessary to re-mesh the model at each advance of the crack tip [22]. The second important observation concerns the post-processing of the stress field found by the finite-element computation around the crack tip. It must be mentioned that with the proposed approach, the assessment of the SIFs and G is made by the interaction integrals, which is rather different from the extrapolation method employed by Kocer in his work.

Thus, in the development of the Hertzian cone model, two main hypotheses are to be considered. The first one concerns the linear elastic behavior assumed for the indented material of the model, which means that plastic deformation is not considered while crack propagation is analyzed. The second important assumption is that the model must have a pre-existing initial crack, positioned at the material's surface and outside the contact region. This predefined flaw is essential for the computation of crack propagation, because the first iteration step requires an initial geometry for the crack path. In Fig. 5, a general representation of the model used in the numerical simulations is given, where the location of the predefined crack (initial flaw) can be appreciated.

This model represents a cylindrical sample loaded by a flat punch, where the crack propagation is evaluated on a meridian section with respect to the indenter axis. The model corresponds to a square of 0.75 mm, composed by regular square elements with the same edge size L_e. Otherwise, the boundary conditions in this model avoid the horizontal displacements of the nodes of the symmetrical axis and the vertical movement of the nodes located on the sample's basis.

As it is presented in Fig. 5, the flat punch radius is $a = 0.1$ mm. Likewise, the initial crack length is defined as $c_f = 0.0325$ mm and the radial position of the initial flaw is $r_o = 0.13$ mm. Moreover, the Young modulus of the indented material corresponds to $E = 70\,000$ MPa and the Poisson ratio is defined as $\nu = 0.2$. As a conclusion, it should be specified that the final crack length for all the numerical simulations is defined as $c = 0.5$ mm.

[1] Let us note here that this crack growth criterion apparently differs from the one used in theoretical investigations (i.e. maximization of G with respect to ϑ). This is particularly true in the context of mixed-mode propagation. But in the context of the cone crack system, it is observed to be almost similar [4].

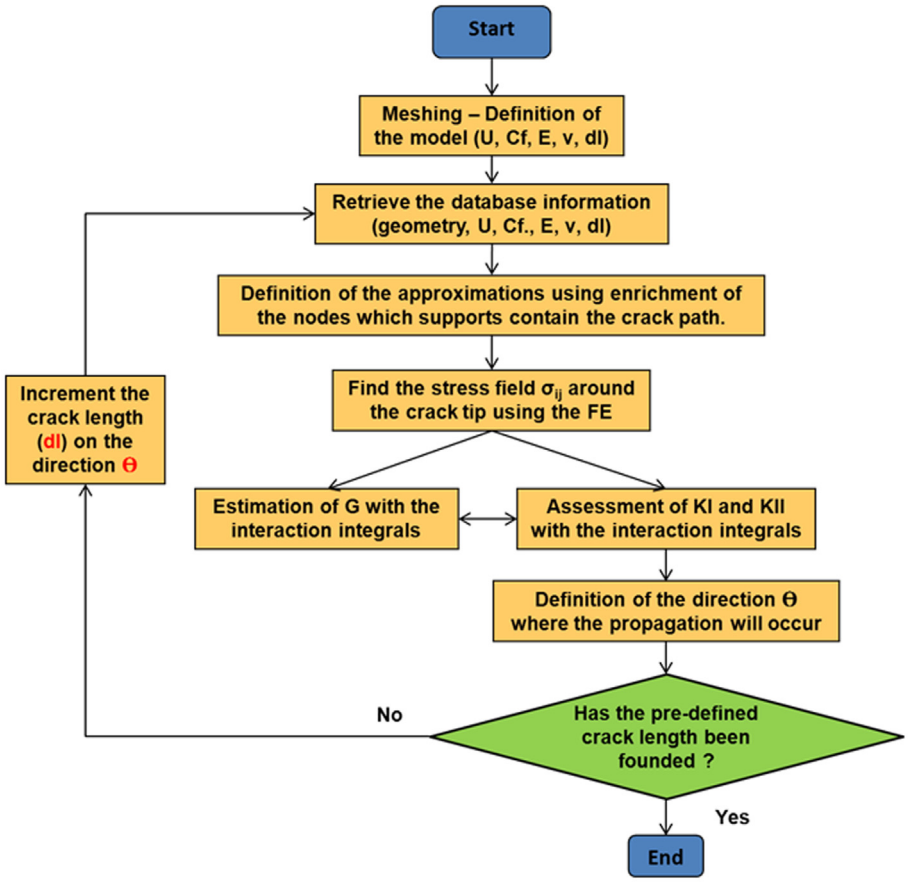

Fig. 4. Description of the numerical simulation of the Hertzian cone using the X-FEM procedure. Color online.

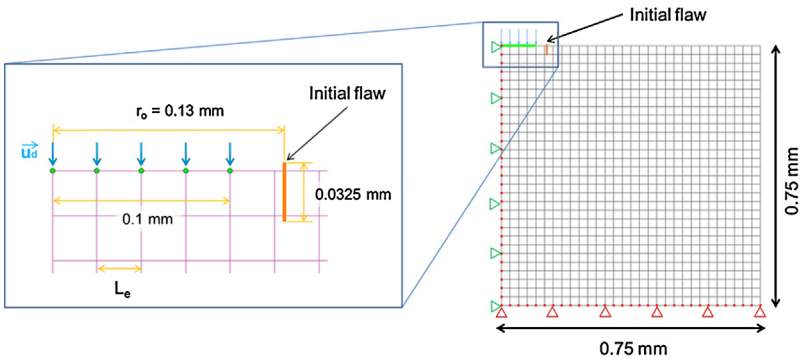

Fig. 5. Model employed for the numerical simulation of the Hertzian cone crack. Color online.

5. Results

In this section, results are compared with the solutions proposed by Kocer and the analytical and experimental descriptions of the Hertzian cone system made by several authors in the past. It is important to keep in mind that the aim of this work is to present the X-FEM procedure as a new alternative in the simulation of Hertzian cone crack propagation, but at the same time, it is the center of discussion on how to discover new interpretations about this phenomenon.

5.1. The Hertzian cone crack path and the measurement of its angle ϑ

Before presenting the results obtained with the X-FEM method, a general approach of the procedure used in the visualization and measurement of the Hertzian crack angle ϑ is exposed. This procedure is based on the use of the level set

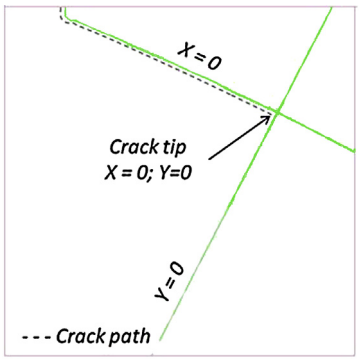

Fig. 6. Visualization of the Hertzian cone crack using the level set functions. Color online.

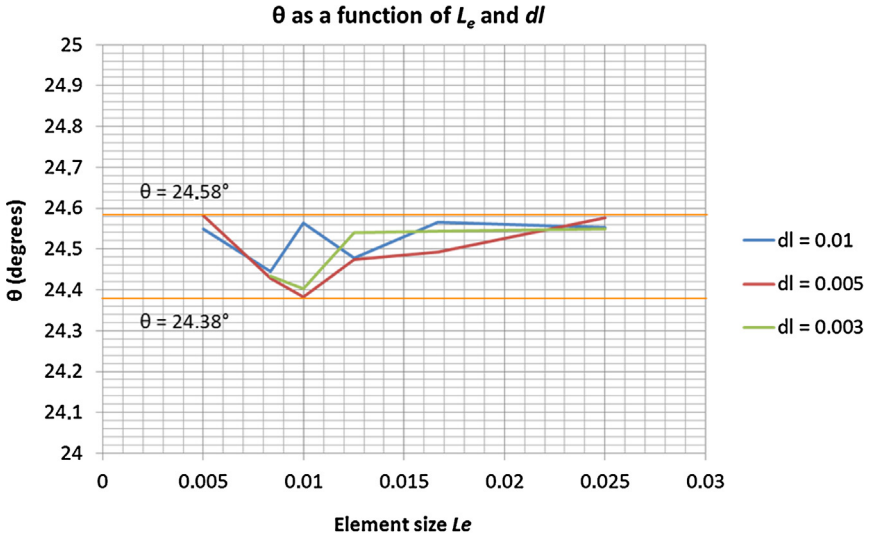

Fig. 7. Influence of the parameters L_e and *dl* on the Hertzian cone angle. Color online.

functions in the representation of the crack path at the last iteration step ($c = 0.5$ mm) [23,24]. In Fig. 6, there is a general description of the process followed. Then, there are two orthogonal family functions (X, Y) from which the crack path is formed by the isovalues "zero" of each function [19,25,26]. The zero-value contour of X represents the cone path and the zero-value contour of Y permits to identify the crack tip at the intersection point of both curves (Fig. 6). Once the crack path is known, the cone crack angle is evaluated with the least square method, identifying the angle of the straight line that best approximates the crack geometry.

5.2. Parameters' influence on the definition of the Hertzian cone

The influence of four parameters is investigated in this section: the mesh element size L_e, the size of the incremental crack step *dl*, the Poisson's ratio ν and the Young modulus E. It should be mentioned that the first two parameters are numerical parameters related to the X-FEM procedure detailed above; meanwhile the other two parameters are associated with the material properties and conditions assumed from the experimental and theoretical analyses.

For constant material conditions ($\nu = 0.2$ and $E = 70\,000$ MPa), 18 numerical simulations were performed for all the possible combinations of six different mesh element sizes L_e (0.025 mm; 0.0166 mm; 0.0125 mm; 0.01 mm; 0.00833 mm; 0.005 mm) and three distinct crack increment values *dl* (0.01 mm; 0.005 mm; 0.003 mm). It should be specified that a shorter crack increment size or a smaller element size obviously entails a higher computation time. The fastest numerical simulation was made in 10 min on a standard Intel(R) Core(TM)2 duo 2.53 GHz PC with 4 Go memory.

The results obtained from this first study are presented in Fig. 7 by means of a graph in which the cone crack angle is related to variables L_e and *dl*. In this diagram, it is possible to observe that the cone angles for all the parameter combinations converge to an average value of 24.5°. Furthermore, it is possible to appreciate that all the solutions are located in a small interval between 24.38° and 24.58°, which means that the cone crack angle is not significantly affected by the variation of those parameters. Otherwise, the solutions obtained are close to the experimental results ($22 \pm 1°$ for $\nu = 0.21$) and the results reached by Kocer [4].

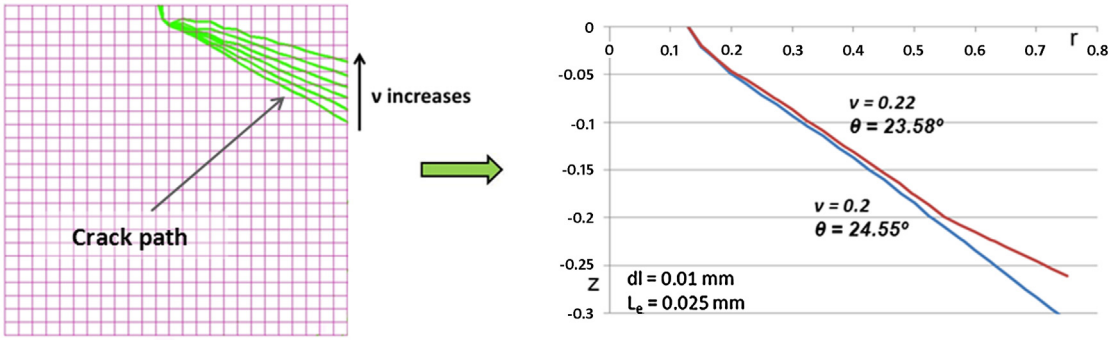

Fig. 8. Influence of the Poisson ratio on the Hertzian cone angle. Color online.

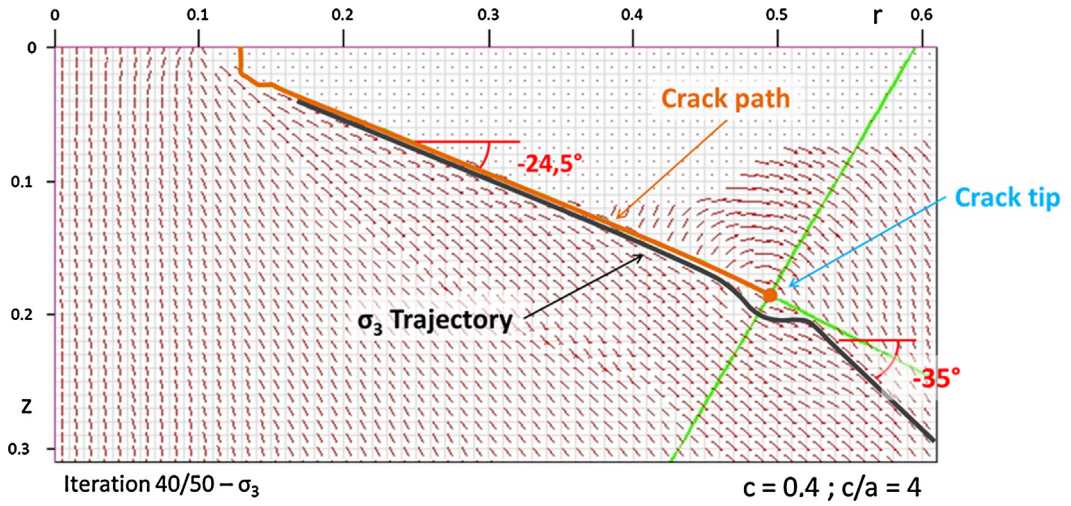

Fig. 9. Distribution of the principal stress direction σ_3 according to the Hertzian cone crack propagation. Color online.

On the other hand, the parameters associated with the material properties were analyzed using a model with a constant mesh size and a constant crack growth increment ($L_e = 0.025$ mm and $dl = 0.01$ mm). In that case, it was possible to remark that the cone angle ϑ decreases when the Poisson ratio ν increases, which corresponds to analytical investigations [2,7]. It is of high interest to observe that the cone angle value is closer to the experimental results when $\nu = 0.22$ than when $\nu = 0.2$ (Fig. 8). Finally, it was observed that the variation of the Young modulus E has no impact on the variation of the crack angle, in good agreement with analytical results.

5.3. The principal stress field on the Hertzian cone system

In the last section, it was proved that the X-FEM is an appropriate technique to model Hertzian cone crack propagation, considering the similarity and coherence between the computed solutions and the experimental results, as well as the comparable material properties used in the numerical model. Thus, in this part of the work, another important feature of the Hertzian cone phenomenon will be analyzed: the principal stress field involved in the Hertzian cone formation and its relation with the crack path geometry. Therefore, for the characterization of the stress influence, only one model from the 18 configurations was employed ($dl = 0.01$ mm and $L_e = 0.01$ mm), because of the negligible influence of those parameters on the determination of the crack angle ϑ. According to the material properties, the Poisson ratio was selected as $\nu = 0.2$ and the Young modulus as $E = 70\,000$.

In Fig. 9, the distribution of principal stress σ_3 direction during crack propagation is presented, as well as the crack path. As the crack faces are submitted to free-surface boundary conditions, crack path-tangent vectors match with the σ_3 direction. Likewise, as previously shown by Kocer [4], the stress direction diverges from the crack path in the regions where the crack did not propagate yet [4,15].

In Fig. 10 is plotted the σ_3 direction and the crack cone angles corresponding to the first and last iteration steps along the crack path. The pre-existing stresses (iteration step 1) converge to 34.4°, whereas the stress direction matches the crack path direction when crack propagates (iteration step 50). These results lead us to state that the principal stresses evolve with crack propagation and the pre-existing stresses are altered from $\sim 35°$ to $\sim 24.5°$, following the crack's orientation.

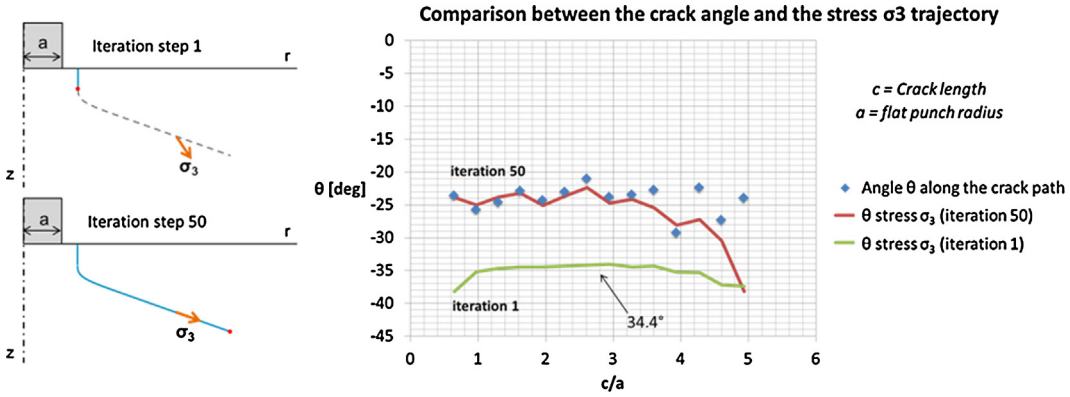

Fig. 10. The minimal principal stress σ_3 orientation before and after the crack tip passage. Color online.

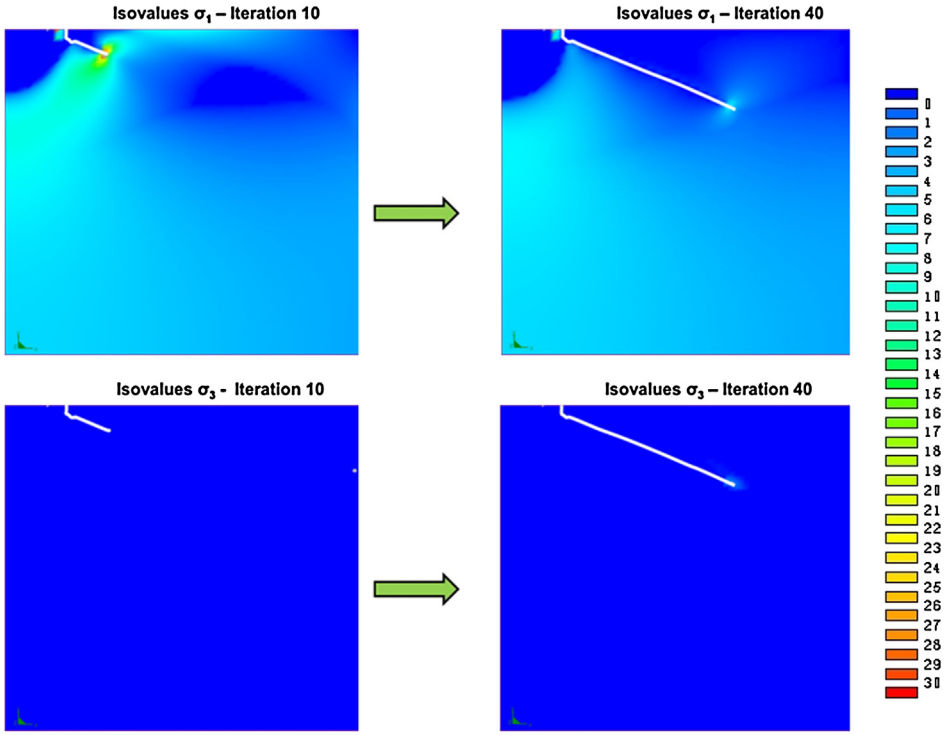

Fig. 11. Distribution of the principal stress σ_1 and σ_3 in MPa at iteration steps 10 and 40. Color online.

In Fig. 11 is plotted the distribution of principal stresses σ_1 and σ_3. Cone crack propagation is observed at two iteration steps (10 and 40), in order to appreciate the crack advancement and the stress variation. In these figures, only the tensile stresses are plotted ($\sigma > 0$), so that the contribution of each stress to the crack propagation can be identified.

From those illustrations, we observe that σ_1 decreases when the crack tip reaches in-depth regions and, as proposed by several authors, all stresses are compressive under the contact region [2,5,7]. Moreover, principal stress σ_3 is compressive everywhere for each iteration step of the crack's advancement (a compressive stress is associated with the dark blue color), which means that this stress does not contribute to the propagation of the cone crack. This assertion is based on the fact that a compressive load cannot generate crack growth. It must be specified here that σ_3 takes positive values at the last iteration, but those values are negligible with respect to the tensile load caused by σ_1. These results lead us to the hypothesis that σ_1 is the only stress that can generate the Hertzian cone propagation, in good agreement with previous theoretical studies [2,7,8].

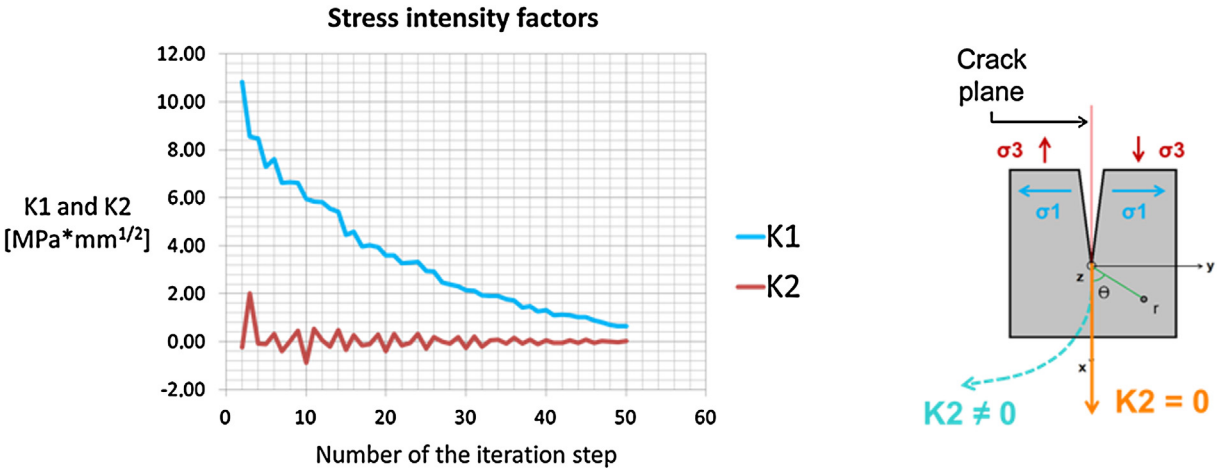

Fig. 12. Stress intensity factors K_1 and K_2 as a function of the crack tip advancement. Color online.

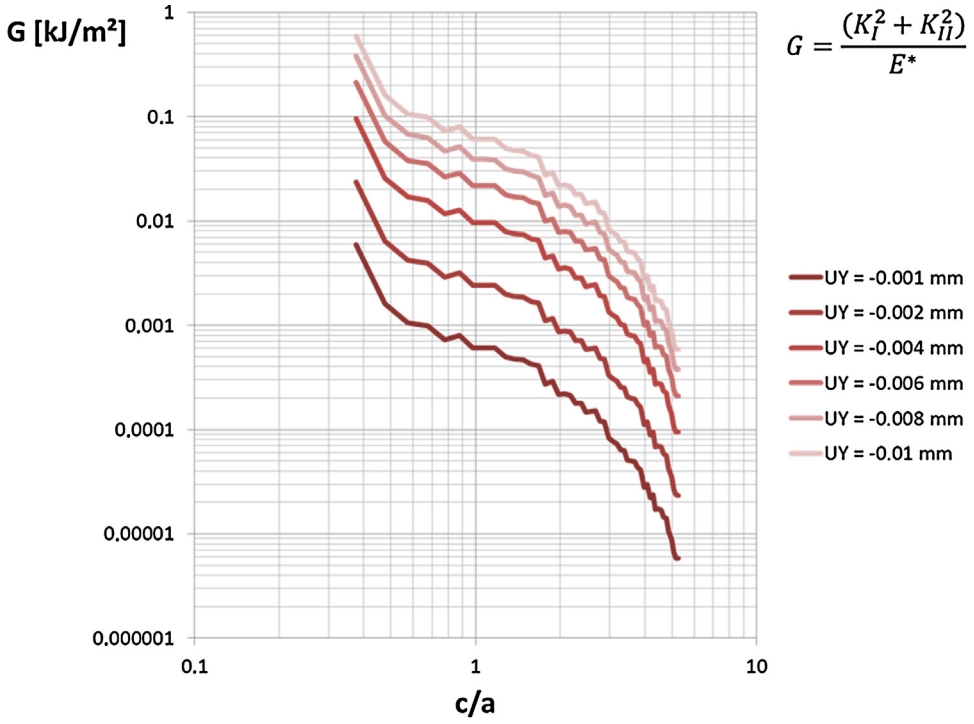

Fig. 13. Strain energy release rate G as a function of normalized crack length c/a.

5.4. The stress intensity factors and the strain energy release rate G

The stress intensity factors (K_1 and K_2) are obtained for each iteration step by the interaction integral technique used in the description of the Hertzian cone crack propagation. In Fig. 12, the variation of each factor as a function of the iteration step is exposed. Factor K_2 is related to a load applied in the tangential direction of the crack plane; meanwhile K_1 corresponds to a normal load to the crack's plane [12]. In this figure, we observe that factor K_2 is negligible with respect to factor K_1, which means that the Hertzian crack propagation is only induced by principal stress σ_1, and propagation follows the crack plane orientation, as indicated in Fig. 12.

With regard to the strain energy release rate, the values of the stress intensity factors are employed for the estimation of G as a function of the normalized crack length c/a (Fig. 13). Each curve of this graphic corresponds to a different indenter penetration distance. From these results, it is appreciable that the Hertzian cone crack propagates in a stable manner (negative slope in the curves) under the effect of a constant indenter load. This graph coincides with the curves proposed by Mouginot and Maugis [2].

6. Conclusion

In this section, we comment upon the most important features related to the numerical simulation performed with the X-FEM technique and the most significant characteristics observed in the Hertzian cone system. First, we will remark that the X-FEM method permits to reach a reliable and accurate representation of the Hertzian cone crack, without employing a re-meshing step and with a reasonable computation-time cost. One interesting result is that the mesh size and the number of iterations do not have a great impact on the crack angle result.

Moreover, the interest of this technique is that there is not a loss of information during stress field computation because the model is never re-meshed, while the iteration process is occurring [16]. In addition to this, we emphasize that the definition of the model on the X-FEM technique is simple and that the visualization of the crack path using the level set functions is pretty useful.

It appears clearly in this paper that the X-FEM technique is very efficient to reproduce faithfully several characteristics of the Hertzian cone crack phenomenon in a very simple manner. More specifically, the crack angle, the strain energy release rate and the stress intensity factors are in good agreement with the solutions proposed in the past. The prediction of the crack angle is in good agreement with experimental data presented in the literature [6,10]. The analysis of the stress field ahead of the crack tip permits to confirm that the trajectories of the minimal principal stress σ_3 evolve according to the crack path extension, from $\sim 35°$ to $\sim 24.5°$ in the regions affected by the crack. Indeed, we appreciate that the cone crack path does not follow the trajectories of the pre-existing stress σ_3 (trajectories defined before the extension of the cone crack) and that it corresponds to the current stress directions.

By the way, these results lead us to formulate a hypothesis about crack propagation: the crack is generated only by the maximum principal stress σ_1, which is orthogonal to the current direction of stress σ_3. This assertion is strongly supported by the results of the SIFs (K_1 and K_2) and the stress field distribution, where σ_3 is compressive for all the iterations steps of the crack growth.

In this work, it is assumed that the indented material remains in the elastic domain. It is now well known [27–29] that even for brittle materials such as silica glasses, indentation-induced plasticity may occur, which could modify the stress field inside the cone crack region. One perspective of our work is to describe the influence of such a plastic flow on the cone crack angle.

Acknowledgements

This work was supported in part by the French National Research Agency (ANR) under contract no. ANR-13-BS09-0012-01. It was also performed within the framework of the LABEX MANUTECH-SISE (ANR-10-LABX-0075) of Université de Lyon, within the program “Investissements d’Avenir” (ANR-11-IDEX-0007).

References

[1] C. Kocer, R.E. Collins, Measurement of very slow crack growth in glass, J. Am. Ceram. Soc. 84 (2006) 2585–2593.
[2] R. Mouginot, D. Maugis, Fracture indentation beneath flat and spherical punches, J. Mater. Sci. 20 (1985) 4354–4376.
[3] A.C. Fischer-Cripps, Predicting Hertzian fracture, J. Am. Chem. Soc. 76 (5) (1997) 1096–1105.
[4] C. Kocer, An automated incremental finite element study of Hertzian cone crack growth, Finite Elem. Anal. Des. 39 (2002) 639–660.
[5] P.D. Warren, D.A. Hills, D.N. Dai, Mechanics of Hertzian cracking, Tribol. Int. 28 (6) (1995) 357–362.
[6] J.J. Benbow, Cone cracks in fused silica, Proc. Phys. Soc. 75 (5) (1960) 697–699.
[7] F.C. Frank, B.R. Lawn, On the theory of Hertzian fracture, Proc. R. Soc. 299 (1967) 291–306.
[8] B.R. Lawn, T.R. Wilshaw, N.E.W. Hartley, A computer simulation study of Hertzian cone crack growth, Int. J. Fract. 10 (1974) 1–16.
[9] C. Kocer, Using a Hertzian fracture system to measure crack growth data: A review, Int. J. Fract. 121 (2003) 111–132.
[10] J.T. Hagan, Cone cracks around Vickers indentations in fused silica glass, J. Mater. Sci. 14 (1979) 462–466.
[11] K.L. Johnson, J.J. O'Connor, A.C. Woodward, The effect of the indenter elasticity on the Hertzian fracture of brittle materials, Proc. R. Soc. A 334 (1973) 95–117.
[12] K. Zeng, K. Breder, D.J. Rowcliffe, The Hertzian stress field and formation of cone cracks – I. Theoretical approach, Acta Metall. Mater. 40 (10) (1992) 2595–2600.
[13] J.L. Swedlow, Criteria for growth of the angled crack, ASTM Special Technical Publication, No. 601, 1976, pp. 506–521.
[14] A. Seweryn, A non-local stress and strain energy release rate mixed mode fracture initiation and propagation criteria, Eng. Fract. Mech. 59 (6) (1998) 737–760.
[15] C. Kocer, R.E. Collins, The angles of Hertzian cone cracks, J. Am. Chem. Soc. 81 (7) (1998) 1736–1742.
[16] N. Moës, J. Dolbow, T. Belytschko, A finite-element method for crack growth without remeshing, Int. J. Numer. Methods Eng. 46 (1) (1999) 131–150.
[17] E. Bechet, H. Minnebo, N. Moës, B. Burgardt, Improved implementation and robustness study of the X-FEM for stress analysis around cracks, Int. J. Numer. Methods Eng. 64 (8) (2005) 1033–1056.
[18] X. Tran, S. Geniaut, Development and industrial applications of X-FEM axisymmetric model for fracture mechanics, Eng. Fract. Mech. 82 (2012) 135–157.
[19] N. Moës, A. Gravouil, T. Belytschko, Non-planar 3D crack growth by the extended finite element and level set. I. Mechanical model, Int. J. Numer. Methods Eng. 53 (11) (2002) 2549–2568.
[20] M. Stolarska, D.L. Chopp, N. Moes, T. Belytschko, Modelling crack growth by level sets in the extended finite element method, Int. J. Numer. Methods Eng. 51 (2001) 943–960.
[21] E. Feulvarch, M. Fontaine, J.-M. Bergheau, XFEM investigation of a crack path in residual stresses resulting from quenching, Finite Elem. Anal. Des. 75 (2013) 62–70.
[22] N. Sukumar, N. Moës, T. Belytschko, B. Moran, Extended finite element method for three dimensional crack modelling, Int. J. Numer. Methods Eng. 48 (11) (2000) 1549–1570.

[23] N. Sukumar, D. Chopp, N. Moës, T. Belytschko, Modeling holes and inclusions by level sets in the extended finite-element method, Comput. Methods Appl. Mech. Eng. 190 (46) (2001) 6183–6200.
[24] J. Sethian, Level Sets Methods and Fast Marching Methods, 2nd ed., Cambridge University Press, 1999.
[25] P. Burchard, L. Cheng, B. Merriman, S. Osher, Motion of curves in three spatial dimensions using level set approach, J. Comput. Phys. 170 (2001) 720–741.
[26] A. Gravouil, N. Moës, T. Belytschko, Non-planar 3D crack growth by the extended finite element and level set. II. Level set update, Int. J. Numer. Methods Eng. 53 (11) (2002) 2569–2586.
[27] E.H. Yoffe, Stress fields of radial shear tractions applied to anelastic half-space, Philos. Mag. A 54 (1986) 553–558.
[28] G. Kermouche, E. Barthel, D. Vandembroucq, P. Dubujet, Mechanical modelling of indentation-induced densification in amorphous silica, Acta Mater. 56 (2008) 3222–3228.
[29] R. Lacroix, G. Kermouche, J. Teisseire, E. Barthel, Plastic deformation and residual stresses in amorphous silica pillars under uniaxial loading, Acta Mater. 60 (2012) 5555–5566.